Applied Acoustics 139 (2018) 174–181

Contents lists available at ScienceDirect

Applied Acoustics

journal homepage: www.elsevier.com/locate/apacoust

A generalized exponential functional link artificial neural networks filter with channel-reduced diagonal structure for nonlinear active noise control

Dinh Cong Le[a,b], Jiashu Zhang[a,*], Defang Li[a], Sheng Zhang[a]

[a] Sichuan Province Key Lab of Signal and Information Processing, Southwest Jiaotong University, Chengdu 610031, PR China
[b] Institute of Engineering and Technology, Vinh University, Viet Nam

ARTICLE INFO

Keywords:
Functional link artificial neural networks
Active noise control
Diagonal-channel structure
Cross-term

ABSTRACT

The nonlinear adaptive exponential functional link artificial neural networks (E-FLANN) filter has been introduced to improve the noise reduction capability of the functional link artificial neural networks (FLANN) in nonlinear active noise control (NANC) system. It, however, suffers from a heavy computational burden at the nonlinear secondary path (NSP) and poor convergence performance in strong nonlinearity systems. To surmount these shortcomings, a computationally efficient generalized E-FLANN filter with the channel-reduced diagonal structure (GE-FLANN-CRD) for NANC system is developed in this paper. Based on introducing the suitable cross-terms and adaptive exponential factor into the trigonometric functional expansions, the nonlinear processing capability of the filter is enhanced in NANC. Also, by applying the filtered-error least mean square (FELMS) algorithm to the GE-FLANN-CRD, it substantially decreases the computational cost to update the exponential factor. Computer simulations demonstrate that the proposed filter-based the NANC system performs better than the FLANN, E-FLANN and Generalized FLANN (GFLANN) filters-based NANC system in the presence of strong nonlinearity.

1. Introduction

To compensate the nonlinear distortions that exist in the actual NANC systems, many researchers have successfully used various nonlinear adaptive filters as the controller. Based on the Volterra filter, bilinear filter, and spline filter, adaptive controllers for NANC system have been proposed in [1–3]. One another method using neural networks (NNs) has also been reported in the literature on NANC, such as multi-layer perceptron (MLP) [4], radial basis function (RBF) [5], the fuzzy neural network [6] and the recurrent neural network (RNN) [7]. Beside, many wavelet frames (such as POLYnominal WindOwed Gaussian (POLYWOG), superposed LOGistic functions (SLOG) and superposed LOGistic functions (SLOG)) have been applied to NANC systems by M Akraminia et al., [8–10]. Apart from those approaches, an efficient alternative based on FLANN using trigonometric functional expansions has received much attention due to its single layer architecture [11–14]. In consequence, various modifiers of FLANN structure for NANC systems have been proposed. Emerging among them can be listed as recursive FLANN (RFLANN) [15], generalized FLANN (GFLANN) [16], bilinear FLANN (BFLANN) [17], convex/cascade combinations of the nonlinear adaptive FLANN filter and other adaptive filters such as the adaptive infinite impulse response (IIR) [18], Volterra [19], FLANN [20] and Legendre polynomial [21].

Recently, in order to further improve the nonlinear modeling capability of the pure sinusoids-based FLANN filter, an adaptive exponential FLANN (E-FLANN) filter has been presented and successfully applied for NANC [22]. In this study, trigonometric functional expansions with the magnitude of the sinusoid are adjusted along with an adaptive exponential factor. However, because of the extra computational cost of filtering the signal through the secondary path to update the exponential factor, its computational complexity increases significantly, especially in the case of NSP. Moreover, in the presence of strong nonlinearity in the secondary or/and primary paths, the performance of the E-FLANN filter may be reduced. This may be caused by the mixed terms with different time delays that exist in the primary and secondary paths under such circumstances (as indicated in [23]). In order to address the aforementioned problems, two improvements are proposed in this paper. Firstly, a generalized E-FLANN with channel-reduced diagonal structure (GE-FLANN -CRD) is presented. It is designed by exploiting suitable cross-terms (the products of input samples at different time delays with trigonometric functions with exponentially varying amplitude) with an implementation based on a diagonal-channel structure. Secondly, a filter-error LMS (FELMS) algorithm is proposed to the GE-FLANN-CRD -based NANC system.

* Corresponding author.
E-mail address: jszhang@home.swjtu.edu.cn (J. Zhang).

https://doi.org/10.1016/j.apacoust.2018.04.020
Received 14 December 2017; Received in revised form 15 March 2018; Accepted 16 April 2018

The rest of this paper is organized as follows. Section 2 proposes GE-FLANN-CRD filter for NANC system. Sections 3 and 4 presents the analysis of computational complexity and stability, respectively. Section 5 provides computer simulation studies of the proposed controller. Finally, the conclusion is drawn in Section 6.

2. Proposed GE-FLANN-CRD filter for NANC system

2.1. The GE-FLANN-CRD filter and its multichannel implementation

An E-FLANN filter of order P, memory length N, using the trigonometric expansion with exponentially varying amplitudes [22] can be described by the input-output relationship as follows

$$y_E(n) = W_E^T(n)X_{EF}(n) \tag{1}$$

where $W_E(n) = [w_{1E}, w_{2E}, \ldots, w_{ME}]^T$ denotes the adaptive weight vector; $[\bullet]^T$ is transpose of a vector; $M = N(2P + 1)$ and $X_{EF}(n)$ is the expanded input signal vector

$$\begin{aligned} X_{EF}(n) = [&x(n), e^{-\beta(n)|x(n)|}\sin(\pi x(n)), e^{-\beta(n)|x(n)|}\cos(\pi x(n)), \ldots \\ &, e^{-\beta(n)|x(n)|}\sin(P\pi x(n)), e^{-\beta(n)|x(n)|}\cos(P\pi x(n)), x(n \\ &-1), e^{-\beta(n)|x(n-1)|}\sin(\pi x(n-1)), e^{-\beta(n)|x(n-1)|}\cos(\pi x(n-1)), \ldots \\ &, e^{-\beta(n)|x(n-1)|}\sin(P\pi x(n-1)), e^{-\beta(n)|x(n-1)|}\cos(P\pi x(n-1)) \ldots \\ &, x(n-N+1), e^{-\beta(n)|x(n-N+1)|}\sin(\pi x(n-N \\ &+ 1)), e^{-\beta(n)|x(n-N+1)|}\cos(\pi x(n-N+1)), \ldots, e^{-\beta(n)|x(n-N+1)|} \\ &\times \sin(P\pi x(n-N+1)), e^{-\beta(n)|x(n-N+1)|}\cos(P\pi x(n-N+1))]^T \end{aligned} \tag{2}$$

where $\beta(n)$ is an adaptive exponential parameter and $X(n) = [x(n)\ x(n-1) \ldots x(n-N+1)]^T$ is the vector of input samples to the E-FLANN filter.

The output of the E-FLANN filter is easily implemented based on a filter bank structure as

$$\begin{aligned} y_E(n) = &\sum_{i=0}^{N-1} a_i(n)x(n-i) + \sum_{i=0}^{N-1} b1_i(n)e^{-\beta(n)|x(n-i)|}\sin(\pi x(n-i)) \\ &+ \sum_{i=0}^{N-1} b2_i(n)e^{-\beta(n)|x(n-i)|}\cos(\pi x(n-i)) \\ &+ \ldots + \sum_{i=0}^{N-1} b(P+1)_i(n)e^{-\beta(n)|x(n-i)|}\sin(P\pi x(n-i)) \\ &+ \sum_{i=0}^{N-1} b(P+2)_i(n)e^{-\beta(n)|x(n-i)|}\cos(P\pi x(n-i)) \end{aligned} \tag{3}$$

where $a_i(n)$, $b1_i(n)$, $b2_i(n)$, $b(P+1)_i(n)$, $b(P+2)_i(n)$ are the corresponding adaptive coefficients.

As discussed above, the performance of the E-FLANN may be degraded in the existence of strong nonlinearity. The main reason may be that its nonlinear extension function lacks cross-terms. To surmount this shortcoming, the cross-terms involving the products of input samples at different time delays with trigonometric functions with exponentially varying amplitudes are introduced into functional expansion. Theoretically, this method can be easily extended to any order $P > 1$. However, to avoid confusion in analysis, in this section we only consider introducing cross-terms into the E-FLANN filter with the order $P = 1$. Hence, a generalized E-FLANN (GE-FLANN) is defined as

$$\begin{aligned} y(n) = &\sum_{i=0}^{N-1} a_i(n)x(n-i) + \sum_{i=0}^{N-1} b1_i(n)e^{-\beta(n)|x(n-i)|}\sin(\pi x(n-i)) \\ &+ \sum_{i=0}^{N-1} b2_i(n)e^{-\beta(n)|x(n-i)|}\cos(\pi x(n-i)) + \sum_{i=0}^{N-1}\sum_{j=1}^{N-1} C1_{i,j}(n)x(n \\ &-i)e^{-\beta(n)|x(n-j)|}\sin(\pi x(n-j)) + \sum_{i=0}^{N-1}\sum_{j=1}^{N-1} C2_{i,j}(n)x(n \\ &-i)e^{-\beta(n)|x(n-j)|}\cos(\pi x(n-j)) \end{aligned} \tag{4}$$

where $C1_{i,j}(n)$ and $C2_{i,j}(n)$ are the coefficients of cross-terms.

Note that the first three components on the right-hand side of the equation above satisfy a time-shift property while the last two components including the cross-terms do not satisfy this property. This results in increasing computational burden when applied to NANC systems. Therefore, we need to consider the diagonal structure feature for the cross-terms, as pointed out in [24–26].

Similar to [26], a GE-FLANN with channel-reduced diagonal structure (GE-FLANN-CRD) is presented as

$$\begin{aligned} y(n) = &\sum_{i=0}^{N-1} a_i(n)x(n-i) + \sum_{i=0}^{N-1} b1_i(n)e^{-\beta(n)|x(n-i)|}\sin(\pi x(n-i)) \\ &+ \sum_{i=0}^{N-1} b2_i(n)e^{-\beta(n)|x(n-i)|}\cos(\pi x(n-i)) \\ &+ sum_{m=1}^{P_r}\sum_{k=0}^{N-m-1} C11_{m,k}(n)x(n-k)e^{-\beta(n)|x(n-m-k)|}\sin(\pi x(n-m \\ &-k)) + \sum_{m=1}^{P_r}\sum_{k=0}^{N-m-1} C12_{m,k}(n)x(n-m-k)e^{-\beta(n)|x(n-k-1)|}\sin(\pi x(n \\ &-k-1)) + \sum_{m=1}^{P_r}\sum_{k=0}^{N-m-1} C21_{m,k}(n)x(n-k)e^{-\beta(n)|x(n-m-k)|}\cos(\pi x(n \\ &-m-k)) + \sum_{m=1}^{P_r}\sum_{k=0}^{N-m-1} C22_{m,k}(n)x(n-m \\ &-k)e^{-\beta(n)|x(n-k-1)|}\cos(\pi x(n-k-1)) \end{aligned} \tag{5}$$

where m denotes the diagonal channel number, k designates the time index, $C11_{m,k}(n)$, $C12_{m,k}(n)$, $C21_{m,k}(n)$ and $C22_{m,k}(n)$ are the coefficients of the cross-terms. Pr is a positive integer and $1 \le P_r \le N-1$. Note that the channels of the cross-terms are defined so that the channel signal sequence satisfies a time-shift property and the diagonal channel number depend on the parameter P_r

To derive the adaptive algorithm for the GE-FLANN-CRD filter, we can rewrite (5) using the vector form as

$$\begin{aligned} y(n) = &A^T(n)U_1(n) + B_1^T(n)U_{21}(n) + B_2^T(n)U_{22}(n) \\ &+ \sum_{m=1}^{P_r} C11_m^T(n)V11_m(n) + \sum_{m=1}^{P_r} C12_m^T(n)V12_m(n) \\ &+ \sum_{m=1}^{P_r} C21_m^T(n)V21_m(n) + \sum_{m=1}^{P_r} C22_m^T(n)V22_m(n) \end{aligned} \tag{6}$$

where the coefficient vector and the corresponding input signal vector are defined by

$$A(n) = [a_0(n)a_1(n) \ldots a_{N-1}(n)]^T \tag{7}$$

$$U_1(n) = [x(n)x(n-1) \ldots x(n-N+1)]^T \tag{8}$$

$$B_1(n) = [b1_0(n)b1_1(n) \ldots b1_{N-1}(n)]^T \tag{9}$$

$$U_{21}(n) = [e^{-\beta(n)|x(n)|}\sin(\pi x(n)) \ldots e^{-\beta(n)|x(n-N+1)|}\sin(\pi x(n-N+1))]^T \tag{10}$$

$$B_2(n) = [b2_0(n)b2_1(n) \ldots b2_{N-1}(n)]^T \tag{11}$$

$$U_{22}(n) = [e^{-\beta(n)|x(n)|}\cos(\pi x(n)) \ldots e^{-\beta(n)|x(n-N+1)|}\cos(\pi x(n-N+1))]^T \tag{12}$$

For $m = 1,2,\ldots,P_r$

$$C11_m^T(n) = [c11_{m,0}(n)c11_{m,1}(n)\ldots c11_{m,N-m-1}(n)]^T \quad (13)$$

$$V11_m^T(n) = [x(n)e^{-\beta(n)|x(n-m)|}\sin(\pi x(n-m))\ldots x(n-N+1+m)e^{-\beta(n)|x(n-N+1)|}\sin(\pi x(n-N+1))]^T \quad (14)$$

$$C12_m^T(n) = [c12_{m,0}(n)c12_{m,1}(n)\ldots c12_{m,N-m-1}(n)]^T \quad (15)$$

$$V12_m^T(n) = [x(n-m)e^{-\beta(n)|x(n-1)|}sin(\pi x(n-1))\ldots x(n-N+1)e^{-\beta(n)|x(n-N+m)|}sin(\pi x(n-N+m))]^T \quad (16)$$

$$C21_m^T(n) = [c21_{m,0}(n)c21_{m,1}(n)\ldots c21_{m,N-m-1}(n)]^T \quad (17)$$

$$V21_m^T(n) = [x(n)e^{-\beta(n)|x(n-m)|}cos(\pi x(n-m))\ldots x(n-N+1+m)e^{-\beta(n)|x(n-N+1)|}cos(\pi x(n-N+1))]^T \quad (18)$$

$$C22_m^T(n) = [c22_{m,0}(n)c22_{m,1}(n)\ldots c22_{m,N-m-1}(n)]^T \quad (19)$$

$$V22_m^T(n) = [x(n-m)e^{-\beta(n)|x(n-1)|}cos(\pi x(n-1))\ldots x(n-N+1)e^{-\beta(n)|x(n-N+m)|}cos(\pi x(n-N+m))]^T \quad (20)$$

Combining the coefficients vectors (7), (9), (11), (13), (15), (17) and (19) we get an overall vector is expressed as

$$W(n) = [A^T(n)B_1^T(n)B_2^T(n)C11_1^T(n)\ldots C11_{Pr}^T(n)C12_1^T(n)\ldots C12_{Pr}^T(n)C21_1^T(n)\ldots C21_{Pr}^T(n)C22_1^T(n)\ldots C22_{Pr}^T(n)]^T \quad (21)$$

Similarly, we can combine (8), (10), (12), (14), (16), (18), and (20) to generalize signal vector $U(n)$ as follows

$$U(n) = [U_1^T(n)U_{21}^T(n)U_{22}^T(n)V11_1^T(n)\ldots V11_{Pr}^T(n)V12_1^T(n)\ldots V12_{Pr}^T(n)V21_1^T(n)\ldots V21_{Pr}^T(n)V22_1^T(n)\ldots V22_{Pr}^T(n)]^T \quad (22)$$

Therefore, the output signal given in (6) can be written in a compact form as

$$y(n) = W^T(n)U(n) \quad (23)$$

As a result, a multichannel structure is implemented for the GE-FLANN-CRD filter as shown in Fig. 1. Clearly, the way to exploit the cross-terms in the GE-FLANN-CRD is different from that given by Sicuranza et al. [16]. In this report, they exploited the cross-terms in a similar way to the diagonal representation of the Volterra filter. However, unlike Volterra filter, it should be noted that these cross-terms do not satisfy symmetry properties.

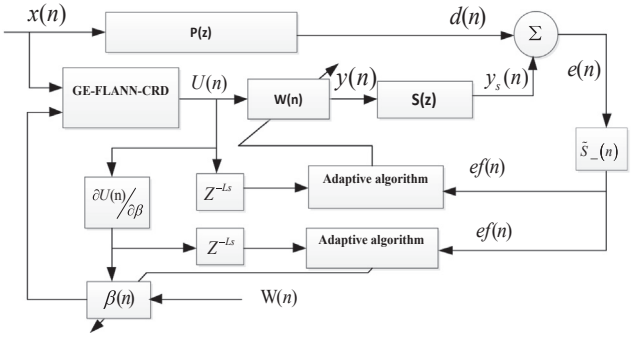

Fig. 2. Adaptive GE-FLANN-CRD filter using FELMS algorithm for NANC system.

2.2. The FELMS algorithm of the adaptive GE-FLANN-CRD filter in NANC systems

According to [22], in order to update the coefficient vector $W(n)$ and the exponential factor $\beta(n)$ of the adaptive E-FLANN filter using the FxLMS algorithm, we must filter the input signals of each parameter ($W(n)$ and $\beta(n)$) through the secondary path. This leads to increased computational complexity. Especially in the case of the secondary path is nonlinear. Although the adaptive exponential factor can enhance the nonlinear processing capability, it increases the computational burden when applied to ANC. To overcome this disadvantage, we propose a filtered-error LMS algorithm for the GE-FLANN-CRD based NANC system, in this section. Its structure is shown in Fig. 2.where $P(z)$ is the transfer function of the primary path, $S(z)$ is the transfer function of the secondary path, $x(n)$ is the reference signal, $d(n)$ is the primary noise sensed at the error microphone, $y(n)$ is the controller output, $y_s(n)$ is the indirectly generated signal at the cancellation point. The GE-FLANN-CRD structure with the adaptive coefficient vector $W(n)$ constitutes the

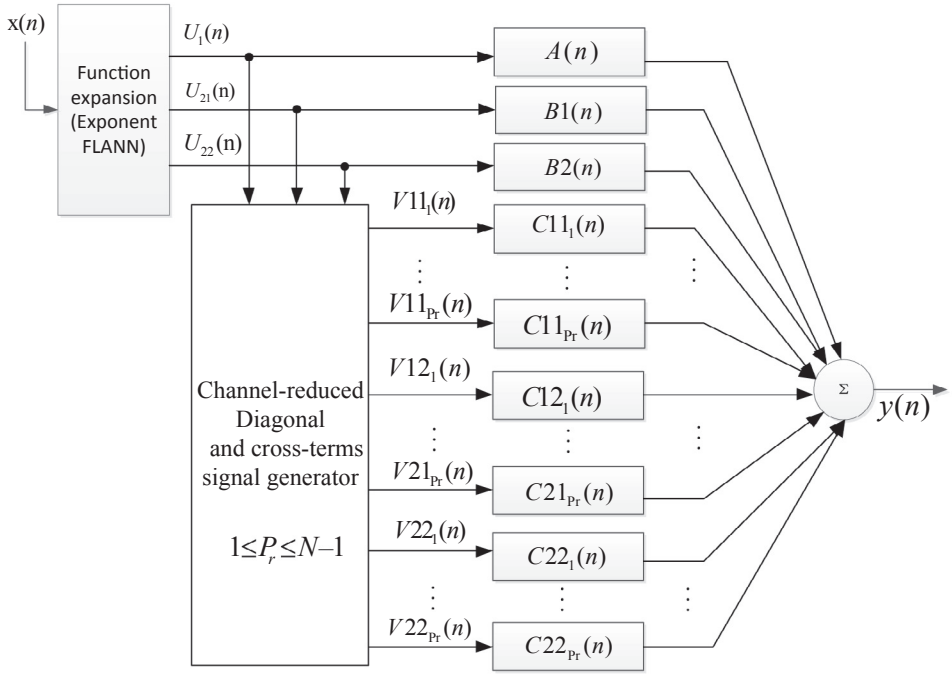

Fig. 1. Multichannel implementation of the GE-FLANN-CRD.

nonlinear controller

For the NANC with linear secondary path (NANC/LSP) system, we can directly apply the algorithms reported in [27,28] to generate the filtered-error based adaptive GE-FLANN-CRD filter. Thus, the update equations of the coefficients vector $W(n)$ and the exponential factor $\beta(n)$ can be expressed as

$$W(n+1) = W(n) + \mu[e(n)*a(n)]U(n-L) \tag{24}$$

$$\beta(n+1) = \beta(n) + \mu_\beta[e(n)*a(n)]W^T(n)U'(n-L) \tag{25}$$

where $a(n)$ represents the error filter which is the transfer function of the estimated secondary path, L denotes the reference signal delay and equal to the length of the estimated secondary path ($L = Ls$), $(*)$ means convolution.

For the NANC with nonlinear secondary path (NANC/NSP) system, since the nature of the secondary path is time-varying, it obstructs the direct application of filtered-error based algorithms to NANC/NSP. Similar to [23], to derive the filtered-error LMS algorithm for adaptive GE-FLANN-CRD filter, we use a concept of a virtual secondary path filter $\widetilde{S}(n)$ with coefficients as

$$\widetilde{S}(n) = [s(n,0)s(n,1)\ldots s(n,Ls)]^T = \left[\frac{\partial y_s(n)}{\partial y(n)}\frac{\partial y_s(n)}{\partial y(n-1)}\ldots\frac{\partial y_s(n)}{\partial y(n-Ls)}\right]^T \tag{26}$$

where Ls is the length of the virtual secondary path.

The coefficient vector $W(n)$ of the nonlinear controller will be adjusted according to the steepest descent algorithm to minimize the instantaneous squared error as follows

$$W(n+1) = W(n) - \frac{1}{2}\mu\nabla_{W(n)}J(n) \tag{27}$$

where μ is the learning rate; $\nabla_{W(n)}J(n)$ is the gradient of cost function $J(n) = E(e^2(n))$ with respect to the weight vector $W(n)$ and is deduced by

$$\nabla_{W(n)}J(n) = \frac{\partial J(n)}{\partial W(n)} = \frac{\partial E(e^2(n))}{\partial W(n)} \cong -2e(n)\frac{\partial y_s(n)}{\partial W(n)} \tag{28}$$

Here, $E(.)$ denotes the expectation operator, $e(n) = d(n) - y_s(n)$ is the residual noise at the error microphone. Note that

$$\frac{\partial y_s(n)}{\partial W(n)} = \sum_{l=0}^{Ls}\frac{\partial y_s(n)}{\partial y(n-l)}\frac{\partial y(n-l)}{\partial W(n)} \tag{29}$$

Assuming that for small step sizes, the weights are slowly varying, then we have

$$\frac{\partial y(n-l)}{\partial W(n)} \approx \frac{\partial y(n-l)}{\partial W(n-l)} = U(n-l) \tag{30}$$

Thus, we can write the update equation of $W(n)$ as

$$W(n+1) = W(n) + \mu e(n)\sum_{l=0}^{Ls} s(n,l)U(n-l) \tag{31}$$

where $s(n,l)$ is the $(l+1)$th component of the virtual secondary path coefficient vector $\widetilde{S}(n)$.

Let $t = n - l + Ls$, so that $n = t + l - Ls$. Thus, the last term in (31), $e(n)\sum_{l=0}^{Ls} s(n,l)U(n-l)$, is expressed as

$$e(n)\sum_{l=0}^{Ls} s(n,l)U(n-l) = [\sum_{l=0}^{Ls} e(t+l-Ls)s(t+l-Ls,l)]U(t-Ls) \tag{32}$$

Let us define vector $\widetilde{S}'(n)$ as a new virtual secondary path filter with coefficients vector as

$$\widetilde{S}'(n) = [s'(n,Ls),s'(n-1,Ls-1),\ldots,s'(n-Ls,0)]^T \tag{33}$$

Note that the vector $\widetilde{S}'(n)$ contrasts with the vector $\widetilde{S}(n)$, it not only requires reversing the order of the coefficients of the vector $\widetilde{S}(n)$ but also requires delaying the time-varying coefficients.

Obviously, the term on the right-hand side of Eq. (32), $\sum_{l=0}^{Ls} e(t+l-Ls)s(t+l-Ls,l)$, can be determined by filtering the error signal $e(n)$ through new virtual secondary path filter $\widetilde{S}'(n)$. Thus, we further define the filtered error as

$$\begin{aligned} ef(n) &= \sum_{l=0}^{Ls} e(n+l-Ls)s(n+l-Ls,l) \\ &= \sum_{l=0}^{Ls} e(n-(Ls \\ &\quad -l)s(n,Ls-l) \end{aligned} \tag{34}$$

where $s'(n,l)$ is the $(l+1)$th component of the vector $\widetilde{S}'(n)$. Combining (31), (32) and (34) we yields

$$W(n+1) = W(n) + \mu ef(n)U(n-Ls) \tag{35}$$

Similarly, the adaptive exponential factor $\beta(n)$ is updated as

$$\beta(n+1) = \beta(n) + \mu_\beta W^T(n)U'(n-Ls)ef(n) \tag{36}$$

where μ_β is the learning rate and $U'(n) = \frac{\partial U^T(n)}{\partial \beta(n)}$

3. Computational complexity analysis

In this section, the comparison of computational complexity of the proposed GE-FLANN-CRD with the GFLANN [16] and the E-FLANN [22] for NANC system are given. Assuming N is memory length, P is the order of sinusoidal expansion function, Ls is the memory size of the secondary path, P_r, N_d are the parameters for the diagonal channel number. When the secondary path is affected by the nonlinearity, it is considered as a time-varying filter. As a result, we cannot take advantage of the delay relationship that exists in the nonlinear state. Conversely, when the secondary path is linear, we can use this delay relationship to reduce the computational burden. Table 1 summarizes the total computational load of the proposed GE-FLANN-CRD, GFLANN [16] and E-FLANN [22] filters for the both NANC/NSP and NANC/LSP case.

Fig. 3a and b illustrate the number of multiplications required in each of the controller for the NANC/NSP and the NANC/LSP, respectively. Assume that the parameters are set to be $N = 10$, $N_d = 9$, $P_r = 2$, $P = 3$ (for E-FLANN), $P = 1$ (for GFLANN and GE-FLANN-CRD), with Ls increasing from 3 to 15. From Fig. 3a, we observed that the E-FLANN and GE-FLANN-CRD using FxLMS algorithm have higher computational complexity than the GFLANN. This result is caused by the extra computational cost for filtering the signal through the secondary path to update the exponential factor. However, thanks to the use of the delay relationship in the case of NANC/LSP, this extra computational cost can be reduced. As shown in Fig. 3b, the computational complexity of the E-FLANN and the GE-FLANN-CRD using the FxLMS algorithm is decreased compared to the computational complexity of the GFLANN. It is evident that the influence of the exponential factor on the computational complexity is considerable, especially in the case of NANC/NSP. Furthermore, Fig. 3 reveals the GE-FLANN-CRD using the FELMS algorithm achieves better computational efficiency. It not only reduces the computation requirement for filtering the signal through the secondary path to update the exponential factor but also the computation requirement for filtering the signal through the secondary path to update the filter coefficients.

4. The analysis of stability conditions

To investigate the stability of the proposed approach, we define a discrete Lyapunov function as

$$P(n) = \frac{e^2(n)}{2} \tag{37}$$

where $e(n)$ is the error signal and P denotes the discrete Lyapunov

Table 1
Comparison of computational complexity for the both NANC/NSP and NANC/LSPcase.

Scheme	FxLMS based E-FLANN [22]		FxLMS based GFLANN[16]		FxLMS based GE-FLANN-CRD		FELMS based GE-FLANN-CRD	
Operations	Mul	Add	Mul	Add	Mul	Add	Mul	Add
Total computational load for NANC/NSP	$(2P+1)N$ $(3+2L_s)+3$	$(2P+1)$ $N(2L_s+1)-1$	$\{P$ $(2NN_d-N_d^2$ $-N_d)+(2$ $P+1)$ $N\}(L_s+2)$ $+2PN_d+1$	$\{P$ $(2NN_d-N_d^2$ $-N_d)+(4$ $P+2)$ $N+(2P+2)$ $PN_d+1)(L_s$ $-1)-1$	$\{(2P+1)$ $N+2P$ $(2NP_r-P_r^2$ $-P_r)\}(2L_s$ $+3)+4P_r$ $P+3$	$\{(2P+1)$ $N+2P$ $(2NP_r-P_r^2$ $-P_r)\}(2L_s$ $+1)-1$	$3\{(2P+1)$ $N+2P(2N$ $P_r-P_r^2-P$ $r)\}+4P_rP$ $+Ls+3$	$3\{(2P+1)$ $N+2P(2$ $NP_r-P_r^2$ $-P_r\}+L$ $s-1$
Total computational load for NANC/LSP	$3(2P+1)$ $N+(4P+2)$ $Ls+3$	$3(2P+1)$ $N+(4P+2)$ $(Ls-1)-1$	$2P$ $(2NN_d-N_d^2$ $-N_d)+(4$ $P+2)$ $N+(2P+2)$ $PN_d+1)$ L_s+2PN_d $+1$	$2P$ $(2NN_d-N_d^2$ $-N_d)+(4$ $P+2)$ $N+(2P+2)$ $PN_d+1)(L_s$ $-1)-1$	$3\{(2P+1)$ $N+2P$ $(2NP_r-P_r^2$ $-P_r)\}+(4$ $P+8P_r+2)$ L_s+4PP_r+3	$3\{(2P+1)$ $N+2P$ $(2NP_r-P_r^2$ $-P_r)\}+(4$ $P+8P_r+2)$ $(L_s-1)-1$	$3\{(2P+1)$ $N+2P(2N$ $P_r-P_r^2-P$ $r)\}+4P_rP$ $+Ls+3$	$3\{(2P+1)$ $N+2P(2$ $NP_r-P_r^2$ $-P_r\}+$ L_s-2

function. During the training process, the change of Lyapunov function can be given by

$$\Delta P(n) = P(n+1) - P(n) = \frac{1}{2}[e^2(n+1) - e^2(n)]$$

from $e(n+1) = e(n) + \Delta e(n)$

$$\Rightarrow \Delta P(n) = \frac{1}{2}\Delta e(n)[2e(n) + \Delta e(n)] \tag{38}$$

For simplicity, we combine the coefficients in the adaptive GE-FLANN-CRD filter for the ANC system as

$$T(n) = [W(n), \beta(n)]^T \tag{39}$$

According to the updating rule developed in this study, $T(n)$ can be adjusted as

$$T(n+1) = T(n) + \Delta T(n) = T(n) - \eta \frac{\partial J(n)}{\partial T(n)}$$

and

$$\Delta T(n) = \eta e(n)\left(\frac{\partial y_s(n)}{\partial T(n)}\right) = \eta e(n) \sum_{i=0}^{Ls-1} s_i \frac{\partial y(n-i)}{\partial T(n)} = \eta e(n) S^* G(n) \tag{40}$$

where $\eta = [\mu, \mu_\beta]$, $S = [s_0, s_1, \ldots s_{Ls}]^T$ is the coefficients of secondary path transfer function and $G(n) = [G_w(n), G_\beta(n)]^T$ are calculated as follows

$$G_w(n) = \left[\frac{\partial y(n)}{\partial a_0} \cdot \cdots \frac{\partial y(n)}{\partial a_{N-1}} \frac{\partial y(n)}{\partial b1_0} \cdot \cdots \frac{\partial y(n)}{\partial b1_{N-1}} \cdot \cdots \frac{\partial y(n)}{\partial b2_0} \cdot \cdots \frac{\partial y(n)}{\partial b2_{N-1}} \frac{\partial y(n)}{\partial c_{11m,0}} \cdot \cdots \frac{\partial y(n)}{\partial c_{11m,N-m-1}} \frac{\partial y(n)}{\partial c_{12m,0}} \cdot \cdots \frac{\partial y(n)}{\partial c_{12m,N-m-1}} \frac{\partial y(n)}{\partial c_{21m,0}} \cdot \cdots \frac{\partial y(n)}{\partial c_{21m,N-m-1}} \frac{\partial y(n)}{\partial c_{22m,0}} \cdot \cdots \frac{\partial y(n)}{\partial c_{22m,N-m-1}}\right]^T \tag{41}$$

$$G_\beta(n) = \frac{\partial y(n)}{\partial \beta} \tag{42}$$

According to the rule of the Taylor expansion, the instantaneous error $e(n)$ is expanded as follows

$$e(n+1) = e(n) + \Delta e(n) = e(n) + \left[\frac{\partial e(n)}{\partial T(n)}\right]^T \Delta T(n) + h.o.t \tag{43}$$

where $h.o.t$ denotes the higher order terms of the rest of Taylor series expansion and can be ignored. Then

$$\Delta e(n) \approx \left[\frac{\partial e(n)}{\partial T(n)}\right]^T \Delta T(n) \tag{44}$$

Substitute (40), (44) in (38) and set $\Delta P(n) < 0$, we have

$$\begin{aligned}\Delta P(n) &= \frac{1}{2}\left[\frac{\partial e(n)}{\partial T(n)}\right]^T \eta e(n) S*G(n)\{2e(n) + \left[\frac{\partial e(n)}{\partial T(n)}\right]^T \eta e(n) S*G(n)\} \\ &= \frac{1}{2}\eta e^2(n)\|Q(n)\|^2\{\eta\|Q(n)\|^2 - 2\} < 0\end{aligned} \tag{45}$$

where $\left[\frac{\partial e(n)}{\partial T(n)}\right]^T = -(S*G(n))^T$, $Q(n) = S*G(n)$, $\|\bullet\|$ is the Euclidean norm and the symbol "$*$" means convolution.

Therefore, the local stability of the system based on the adaptive GE-FLANN-CRD filter is guaranteed provided that $0 < \eta < 2/\|Q(n)\|^2$.

5. Simulations

In order to prove the effectiveness of the proposed GE-FLANN-CRD filter for the NANC systems, four scenarios of nonlinear ANC system are simulated in this section. And to provide a fair comparison, all adaptive filters including FLANN, E-FLANN, GFLANN and GE-FLANN-CRD are updated by FxLMS-based algorithms. Also, to demonstrate computational efficiency of the proposed filter, the GE-FLANN-CRD updated by

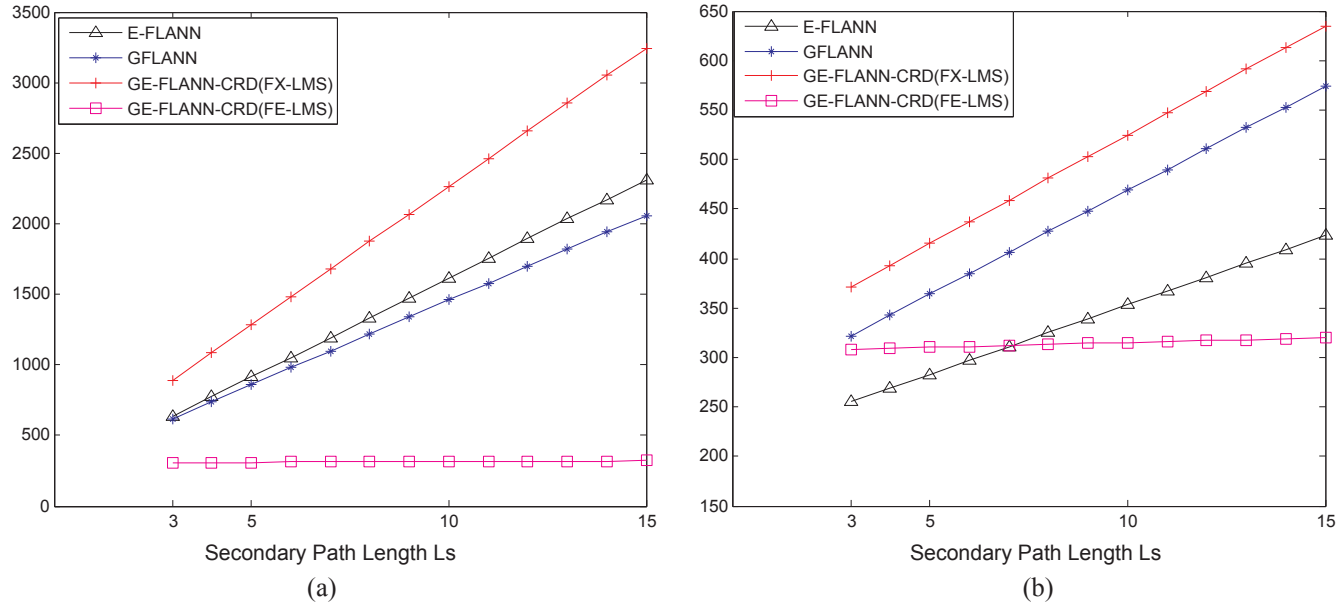

Fig. 3. Illustrate the number of multiplications required in each of the controller for (a) NANC/NSP and (b) NANC/LSP.

a FELMS-based algorithm is also compared.

The memory length of the all filters are chosen as $N = 10$. The function expansion of the input signal is third-order type ($P = 3$) for the FLANN, E-FLANN and first-order type ($P = 1$) for GFLANN and GE-FLANN-CRD. The number of diagonal channels of the GE-FLANN-CRD and GFLANN is chosen as $P_r = 2$ and $N_d = 9$, respectively. The performance of the different filters is measured in terms of the normalized mean square error (NMSE) which obtained by averaging over 100 independent runs.

5.1. Experiment 1

In this experiment, the reference noise $x(n)$ is a sinusoidal wave of 500 Hz sampled at the rate of 8000 samples/s, which is obtained by $x(n) = \sqrt{2}\sin(2\pi 500n/8000) + v(n)$, and $v(n)$ denotes a Gaussian noise of 40 dB SNR. The primary noise observed at the cancellation point is assumed as the following third-order polynomial model $d(n) = t(n-2) + g_1 t^2(n-2) - g_2 t^3(n-2)$. where g_1, g_2 are a measure of the strength of the primary path nonlinearity, $t(n) = x(n) * f(n)$ and $f(n)$ is the impulsive response of the transfer function $f(z) = z^{-3} - 0.3z^{-4} + 0.2z^{-5}$.

Case 1: The secondary path is the non-minimum phase with a transfer function as $S(z) = z^{-2} + 1.5z^{-3} - z^{-4}$. The strength of the primary path nonlinearity is chosen as a weak nonlinear distortion case: $g_1 = 0.08$, $g_2 = 0.04$. The learning rate of FLANN is set to $\eta 1_w = 0.007$, $\eta 1_H = 0.003$ for the linear and nonlinear parts, respectively. The learning rate of E-FLANN is set to$\eta 2_w = 0.0065$, $\eta 2_H = 0.003$ and $\beta_2 = 0$ for the linear, nonlinear parts and the adaptive exponential factor, respectively. Learning rate of GFLANN are $\eta 3_w = 0.006$, $\eta 3_H = 0.0025$ and $\eta 3_c = 0.0005$ for the linear, the sin(.) cos(.) functions and the cross-terms parts, respectively. The learning rate of GE-FLANN-CRD uses FxLMS algorithm as $\mu 1_a = 0.0045$, $\mu 1_b = 0.0015$, $\mu 1_c = 0.0008$ and $\beta_X = 0$ for the linear, the sin(.) cos(.) functions, the cross-terms parts and the adaptive exponential factor, respectively. The learning rate of GE-FLANN-CRD uses FELMS algorithm as $\mu 2_a = 0.006$, $\mu 2_b = 0.0025$, $\mu 2_c = 0.0005$ and $\beta_E = 0$ for the linear, the sin(.) cos(.) functions, the cross-terms parts and the adaptive exponential factor, respectively. Fig. 4 depicts the performance comparison of NMSE for the FLANN, E-FLANN, GFLANN and GE-FLANN-CRD controllers in weak nonlinear distortion case.

Case 2: The strength of the primary path nonlinearity is chosen as a strong nonlinear distortion case: $g_1 = 0.8$, $g_2 = 0.4$. The secondary path is chosen similarly to *case* 1. The learning rates of the different filters used as: for the FLANN ($\eta 1_w = 0.005$, $\eta 1_H = 0.002$); for the E-FLANN ($\eta 2_w = 0.0008$, $\eta 2_H = 0.0004$ and $\beta_2 = 0.02$); for the GFLANN ($\eta 3_w = 0.005$, $\eta 3_H = 0.0015$; $\eta 3_c = 0.001$); for the GE- FLANN-CRD using FxLMS ($\mu 1_a = 0.0009$, $\mu 1_b = 0.0005$, $\mu 1_c = 0.0003$ and $\beta_X = 0.01$); for the GE-FLANN-CRD using FELMS ($\mu 2_a = 0.001$, $\mu 2_b = 0.0006$, $\mu 2_c = 0.0003$ and $\beta_E = 0.01$).

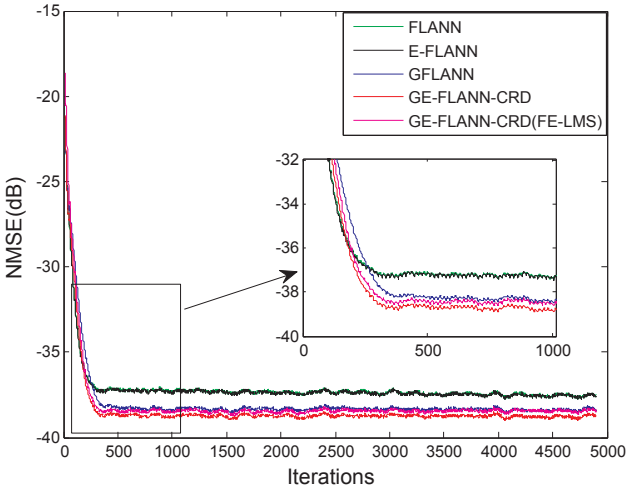

Fig. 4. Performance comparisons with weak nonlinearity in the primary path, non-minimum phase secondary path.

Fig. 5a illustrates the NMSE performance curves of the filters for the nonlinear ANC systems in strong nonlinear distortion case. Fig. 5b represents the change in the adaptive exponential factor with respect to iterations.

Case 3: The secondary path transfer function is chosen to be the minimum-phase model $S(z) = z^{-2} + 0.5z^{-3}$. Table 2 summarizes simulation results for both cases: the primary path contains strong nonlinear distortion and weak nonlinear distortion. Here, the NMSE values are measured after 5000 iterations at the same initial convergence speed.

From Figs. 4, 5a and Table 2, it is evident that the GE-FLANN-CRD exhibits better performance in comparison with FLANN, E-FLANN and

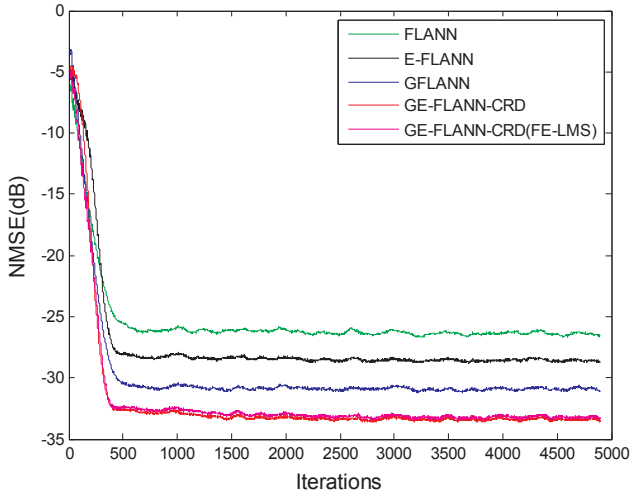

Fig. 5a. Performance comparisons with strong nonlinearity in the primary path, non-minimum phase secondary path.

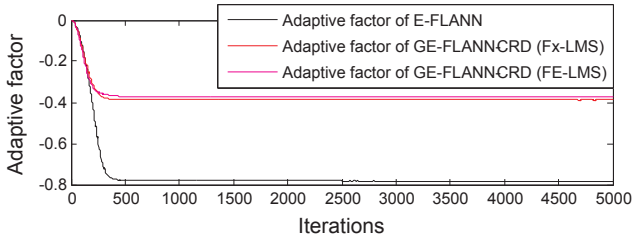

Fig. 5b. Variation of the adaptive exponential factor.

Table 2
The NMSEs of different filters for nonlinear ANC.

Controllers	weak nonlinearity	strong nonlinearity
FLANN	−36.61 dB	−24.18 dB
E-FLANN	−36.61 dB	−26.58 dB
GFLANN	−38.14 dB	−30.68 dB
GE-FLANN-CRD	−39.05 dB	−33.15 dB
GE-FLANN-CRD (FE-LMS)	−39.02 dB	−33.15 dB

GFLANN. And the performance of the GE-FLANN-CRD using the FELMS algorithm is equivalent to that of the GE-FLANN-CRD using the FxLMS algorithm. In addition, in the case of the strong nonlinear distortion, the proposed GE-FLANN-CRD filter achieves superior performance over the FLANN, E-FLANN and GFLANN filters.

5.2. Experiment 2

In practical ANC system, the main components such as the power amplifier and loudspeaker at the output of the filter can be considered as a secondary path. It is usually approximated by block-oriented nonlinear models that are the Wiener, Hammerstein, and linear–-memoryless nonlinear–linear (LNL) cascade models.

In this experiment, we use the secondary path as the Hammerstein model with a memoryless nonlinearity $v(n) = \tanh(y(n))$ and followed by filter $y_s(n) = v(n) + 0.2v(n-1) + 0.05v(n-2)$. The primary path is assumed as high nonlinear behavior and modeled by a Volterra series $d(n) = x(n) + 0.8x(n-1) + 0.3x(n-2) + 0.4x(n-3) - 0.8x(n)x(n-1) + 0.9x^2(n-2) + 0.7x^2(n-3) - 3.9x^3(n-1) - 2.6x^2(n-1)x(n-3) + 2.1x^2(n-2)x(n-3)$. The reference signal is colored noise that are generated from autoregressive moving average models by filtering a random sequence through $x(n) = 0.04x(n-1) - 0.034x(n-2) + 0.0396x(n-3) - 0.07565x(n-4) - 0.1u(n) - 0.01u(n-1) - 0.137u(n-2) + 0.0353u(n-3) + 0.0698u(n-4)$, where $u(n)$ is mean-zero white Gaussian sequence with variance one. The learning rates of the different filters are: for the FLANN ($\eta 1_w = 0.01$, $\eta 1_H = 0.005$); for the E- FLANN ($\eta 2_w = 0.03$, $\eta 2_H = 0.005$ and $\beta_2 = 0.1$); for the GFLANN ($\eta 3_w = 0.07$, $\eta 3_H = 0.01$; $\eta 3_c = 0.03$); for the GE-FLANN-CRD using FxLMS ($\mu 1_a = 0.07$, $\mu 1_b = 0.02$, $\mu 1_c = 0.03$ and $\beta_X = 0.08$); for the GE-FLANN-CRD using FELMS ($\mu 2_a = 0.05$, $\mu 2_b = 0.015$, $\mu 2_c = 0.03$ and $\beta_E = 0.051$).

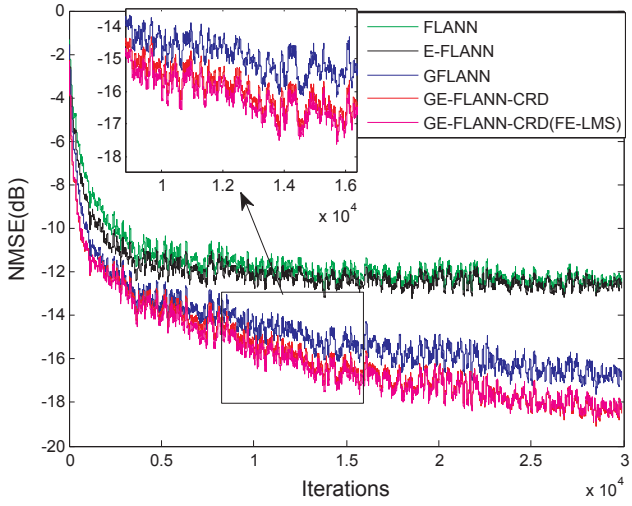

Fig. 6. Performance comparison of different controllers using the secondary path as the Hammerstein model.

Fig. 6 shows a comparative plot of the NMSE achieved by the NANC systems with the FLANN, E-FLANN, GFLANN and GE-FLANN-CRD filters for the case of the secondary path approximated by the Hammerstein model. From Fig. 6, it is observed that the proposed GE-FLANN -CRD filter using the FELMS or FxLMS algorithm yield better NMSE performance compared to the FLANN, E-FLANN and GFLANN.

5.3. Experiment 3

In this experiment, we assume that the secondary path is modeled by a volterra series whose input and output relationship is described as $y_s(n) = y(n) + 0.35y(n-1) + 0.09y(n-2) - 0.5y(n)y(n-1) + 0.4y(n)y(n-2)$. The primary path is chosen as the one used in experiment 2. The reference signal is random noise with a uniform distribution between −0.5 and +0.5. The learning rate for all the filters are chosen as: the FLANN ($\eta 1_w = 0.003$, $\eta 1_H = 0.0005$); the E-FLANN ($\eta 2_w = 0.005$, $\eta 2_H = 0.0005$ and $\beta_2 = 0.02$); the GFLANN ($\eta 3_w = 0.065$, $\eta 3_H = 0.02$; $\eta 3_c = 0.02$); the GE-FLANN-CRD using FxLMS ($\mu 1_a = 0.028$, $\mu 1_b = 0.002$, $\mu 1_c = 0.012$ and $\beta_X = 0.008$); the GE-FLANN-CRD using FELMS ($\mu 2_a = 0.018$, $\mu 2_b = 0.001$, $\mu 2_c = 0.01$ and $\beta_E = 0.008$).

Fig. 7 shows the simulation result when the secondary path and the primary path are time-varying nonlinear models. It is evident that the GE-FLANN-CRD using the FELMS or FxLMS algorithm exhibits better performance in comparison with FLANN, E-FLANN and GFLANN.

6. Conclusion

In this paper, we proposed the computationally efficient GE-FLANN-CRD filter to improve the noise mitigation capability of the E-FLANN in nonlinear ANC system. The performance of the filter has been enhanced by exploiting the suitable cross-terms and adaptive exponential factor. Based on the diagonal-channel structure, this GE- FLANN-CRD filter is easily implemented with the filter bank form. Moreover, computational complexity and stability analysis has revealed that the FELMS algorithm derived is suitable for GE-FLANN-CRD. Finally, the simulation

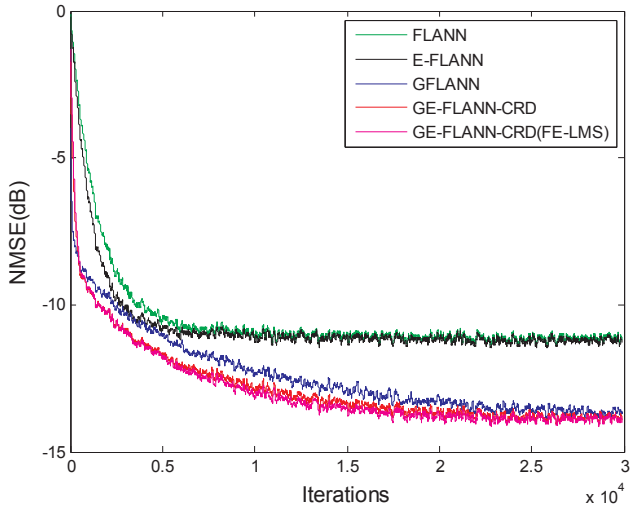

Fig. 7. Performance comparison of different controllers using the secondary path as the volterra model.

results have confirmed that for the NANC with strong nonlinearity, the proposed GE-FLANN-CRD filter offers better control performance than the FLANN, E-FLANN and GFLANN filters.

Funding

This work was partially supported by National Science foundation of P. R. China (Grant: 61671392) and by the Fund for the Basic Research Program of Sichuan province, China (Grant: 2013JY0036).

References

[1] Tan L, Jiang J. Adaptive Volterra filter for active control of nonlinear noise processes. IEEE Trans Signal Process 2001;49(8):1667–76.
[2] Kuo SM, Wu HT. Nonlinear adaptive bilinear filters for active noise control systems. IEEE Trans Circuits Syst.-I: Regular Papers 2005; 52(3): 617–24.
[3] Patel V, George NV. Nonlinear active noise control using spline adaptive filters. Appl Acoust 2015;93:38–43.
[4] Snyder SD, Tanaka N. Active control of vibration using a neural network. IEEE Trans Neural Networks 1995;6:819–28.
[5] Tokhi MO, Wood R. Active noise control using radial basis function networks. Control Eng Practice 1997;5(9):1311–22.
[6] Zhang QZ, Gan WS, Zhou YL. Adaptive recurrent fuzzy neural networks for active noise control. J Sound Vib 2006;296(4):935–48.
[7] Bouchard M, Pailard B, Dinh CTL. Improved training of neural networks for non-linear active control of sound and vibration. IEEE Trans Neural Networks 1999;10(2):391–401.
[8] Akraminia M, Mahjoob MJ, Tatari M. Active noise control using adaptive POLYnomial Gaussian WinOwed wavelet networks. J Vib Control 2014;21(15):3020–33.
[9] Akraminia M, Mahjoob MJ. Adaptive feedback active noise control using wavelet frames: simulation and experimental results. J Vib Control 2014;22:1895–912.
[10] Akraminia M, Mahjoob MJ, Niazi AH. Feedforward active noise control using wavelet frames: simulation and experimental results. J Vib Control 2015;23:555–73.
[11] Das DP, Panda G. Active mitigation of nonlinear noise processes using a novel filtered-s LMS algorithm. IEEE Trans Speech Audio Process 2004;12(3):313–22.
[12] George NV, Panda G. A robust filtered-s LMS algorithm for nonlinear active noise control. Appl Acoust 2012;73:836–41.
[13] Behera SK, Das DP, Subudhi B. Adaptive nonlinear active noise control algorithm for active headrest with moving error microphones. Appl Acoust 2017;123:9–19.
[14] Zhao HQ, Zhang JS. Functional link neural network cascaded with Chebyshev orthogonal polynomial for nonlinear channel equalization. Signal Process 2008;88:1946–57.
[15] Sicuranza GL, Carini A. On the BIBO stability condition of adaptive recursive FLANN filters with application to nonlinear active noise control. IEEE Trans Audio Speech Lang Process 2012;20(1):234–45.
[16] Sicuranza GL, Carini A. A generalized FLANN filter for nonlinear active noise control. IEEE Trans Audio Speech Lang Process 2011;19(8):2412–7.
[17] Le DC, Zhang JS, Pang YJ. A bilinear functional link artificial neural network filter for nonlinear active noise control and its stability condition. Appl Acoust 2018;132:19–25.
[18] George NV, Panda G. On the development of adaptive hybrid active noise control system for effective mitigation of nonlinear noise. Signal Process 2012;92(2):509–16.
[19] George NV, Gonzalez A. Convex combination of nonlinear adaptive filters for active noise control. Appl Acoust 2014;76:157–61.
[20] Zhao HQ, Zeng XP, He ZY, Yu SJ, Chen BD. Improved functional link artificial neural network via convex combination for nonlinear active noise control. Appl Soft Comput 2016;42:351–9.
[21] George NV, Panda G. Active control of nonlinear noise processes using cascaded adaptive nonlinear filter. Appl Acoust 2014;74:217–22.
[22] Patel V, Gandhi V, Heda S, George NV. Design of adaptive exponential functional link network-based nonlinear filters. IEEE Trans Circuits, Syst. I 2016; 63(9): 1434–42.
[23] Zhou D, Brunner V. Efficient adaptive nonlinear filters for nonlinear active noise control. IEEE Trans Circuits Syst.-I 2007; 54(3): 669–81.
[24] Tan L, Jiang J, Wang L. Adaptive diagonal-channel bilinear filters for nonlinear active noise control. Int J Control Sci Eng 2014;4(2):27–35.
[25] Zhao H, Zeng X, He Z, Li T, Jin W. Nonlinear adaptive filter-based simplified bilinear model for multichannel active control of nonlinear noise processes. Appl Acoust 2013;74(12):1414–21.
[26] Tan L, Dong C, Du S. On implementation of adaptive bilinear filters for nonlinear active noise control. Appl Acoust 2016;106:122–8.
[27] Miyagi S, Sakai H. Mean-square performance of the filtered- reference/filtered-error LMS algorithm. IEEE Trans Circuits Syst.–I: Regular pap 2005; 52 (11): 2454–63.
[28] Brunner V, Zhou D. Hybrid filtered error LMS algorithm: another alternative to filtered-x LMS, IEEE Trans Circuits Syst.–I: Regular Pap 2006; 53 (3): 653–61.